

EFFECT OF ZnO NANOPOWDER SOURCE AND GROWTH TEMPERATURE ON SHAPE EVOLUTION OF ZnO NANOSTRUCTURES

SOUMEN DHARA* and P. K. GIRI*^{†,‡}

**Department of Physics,*

*[†]Centre for Nanotechnology, Indian Institute of Technology
Guwahati, Guwahati-781 039, India*

[‡]giri@iitg.ernet.in

Received

Accepted

We study the effect of ZnO source and growth temperatures on morphology of the ZnO nanostructures. Nanostructures grown from ZnO nanopowder show the shape evolution from nanowires to nanoribbons and then to nanorods with variation in growth temperature and zinc vapor pressure. At 750°C, only vertically aligned nanowires have been observed and with increase in growth temperature nanowires transforms to nanoribbons and then finally to nanorods at 870°C. On the other hand, in case of ZnO bulk powder as a source material, only nanowires are produced at all temperatures. Raman scattering studies on the nanostructures show distinct E_2^{high} mode at $\sim 437 \text{ cm}^{-1}$, confirming the hexagonal wurtzite phase of the as grown nanostructures. Room temperature photoluminescence spectra exhibit bound exciton related strong UV emission at $\sim 379 \text{ nm}$ indicating high quality of the as-grown nanostructures. Possible mechanism of growth and shape evolution in ZnO nanostructures are explored through systematic studies of the effect of growth temperatures and zinc vapor pressure.

Keywords: ZnO nanowires; shape evolution; ZnO nanopowder source; vapor-liquid-solid growth.

1. Introduction

ZnO is one of the important functional materials that have wide applications in the field of optoelectronics to mechanical actuators and sensors.¹ Wide band gap (3.37 eV), large exciton binding energy (60 meV at room temperature), lack of centre of symmetry in wurtzite structure, easy growth process of varieties of nanostructures are the key factors of ZnO for getting intense research attention.² ZnO nanostructures have attracted much attention owing to its application to various nanodevices from light emitting diodes to solar cells.^{3–6} Each nanostructure is suitable for use in

specific nanodevices. Nanorods and straight nanowires are suitable for use in laser, nanowires are suitable for sensors and transistors, nanobelts are useful for use in transducers and actuators. ZnO has a diverse group of growth morphologies, such as rods, wires, ribbons, belts, tetrapods etc.¹ For the ZnO nanodevice application, it is important to have the ability to control the shape, size and orientation of the nanostructures. It is generally believed that source material, growth temperature and vapor pressure concentration strongly control the final shape and size of the nanostructures. Ye *et al.*⁷ have studied morphology derivation of ZnO

nanostructures from nanoplatelets to nanowires using ZnO bulk powder as the source material by vapor-solid (VS) growth process. In this work, we study the effect of ZnO nanopowder source and growth temperatures on morphology of the ZnO nanostructures. It is shown that as grown nanostructures undergo shape evolution with variation in growth temperature and zinc vapor pressure. Mechanism of shape evolution is discussed.

2. Experimental Details

Various ZnO nanostructures were synthesized in a horizontal muffle furnace using a quartz tube by a vapor deposition method using gold catalyst. Commercial ZnO nanopowder (Sigma-Aldrich, purity 99.999%, grain size was measured by dynamic light scattering technique $\sim 50\text{--}70\text{ nm}$) was mixed with high purity graphite powder (Fluka) in 1:1 weight ratio, and that mixture was used as source material for deposition. Then mixture was placed at the center of the furnace inside the quartz tube and heated to 950°C for 30 min. About 2 nm gold layer was deposited by sputtering process on the cleaned Si(100) substrate for catalyst assisted growth and it was placed at elevated temperature zones of the furnace inside the quartz tube. Ar gas was used as vapor carrier gas with a flow rate of 70 sccm. For comparison, ZnO bulk powder (Sigma-Aldrich, purity 99.999%) was used as the source material for studying the growth process.

After deposition, structure and morphology of the grayish-black samples were analyzed using scanning electron microscope (SEM, LEO 1430VP), transmission electron microscope (TEM, JEOL JEM2100) and X-ray diffraction with Cu K_α radiation (XRD, Seifert 3003 T/T). Photoluminescence (PL) property of these nanostructures was directly measured under excitation of 325 nm laser at room temperature using a commercial fluorimeter (Edinburg, FS-920P). Phonon modes were studied using a micro-Raman spectrometer with Ar^+ laser (Jobin Yvon, LabRam HR800).

3. Results and Discussion

Figures 1(a)–1(c) show various nanostructures grown from ZnO nanopowder source. The shape of the nanostructures vary from nanowires to nanoribbons and then to nanorods with decreasing the distance between source and substrate. Vertically

aligned dense nanowires were grown on the gold coated substrate placed at 750°C (Fig. 1(a)). These nanowires have diameter 40–55 nm and length about few microns. Figure 1(b) shows the growth of dense and long nanoribbons at 850°C , which is closer to the source material than the previous case. The nanoribbons have length of more than $10\ \mu\text{m}$ and width 300–500 nm. The nanoribbons are tapered shaped with smallest tip size about 40 nm. At 870°C , which is nearer to the source material, we observed the formation of dense nanorods with hexagonal facet (Fig. 1(c)). The nanorods are found to be vertically aligned. The diameter of the nanorods varies from 200–300 nm and length of several microns. On the other hand, in case of ZnO bulk powder as a source material, only nanowires are produced, which have different length and diameter depending upon the growth temperatures. Figure 1(d) shows the nanowires grown at 750°C using ZnO bulk powder as source. The diameter of the nanowires at the top edge is 30–70 nm and 110–160 nm at the bottom side and length about 2–4 μm . This is a large estimation of diameter of the nanowires due to non-uniformity. The nanowires grown at higher temperature shows larger diameter and length. Therefore, we observed temperature dependent shape evolution of ZnO nanowires, when ZnO nanopowder is used as the source material. At lower temperature and lower zinc vapor pressure, nanowires were formed and then transformed towards nanoribbons and then to nanorods at high temperature region and higher vapor pressure.

We examined the crystal structure of the as-grown ZnO nanostructures by XRD. The XRD patterns (not shown) of all the nanostructures show one strong peak at 34.4° with FWHM $\sim 0.280^\circ$ and a very weak peak at 62.7° . These peaks are corresponding to (002) and (103) planes of hexagonal ZnO. The XRD results show that the ZnO nanostructures are grown along c -axis of hexagonal structures.

The ZnO nanostructures were further investigated by employing TEM and SAED. Figures 2(a)–2(c) show the typical TEM images of nanowires, nanoribbons and nanorods, respectively. SAED pattern of the nanowire is shown in Fig. 2(d), which can be indexed to $10\bar{1}0$ zone axis of the wurtzite ZnO. The SAED pattern confirms single crystalline growth along $\langle 0002 \rangle$ direction. HRTEM images (Figs. 2(e) and 2(f)) of the nanowire and nanorod does not show any extended defects in the crystal structure. The inter planner spacing is approximately

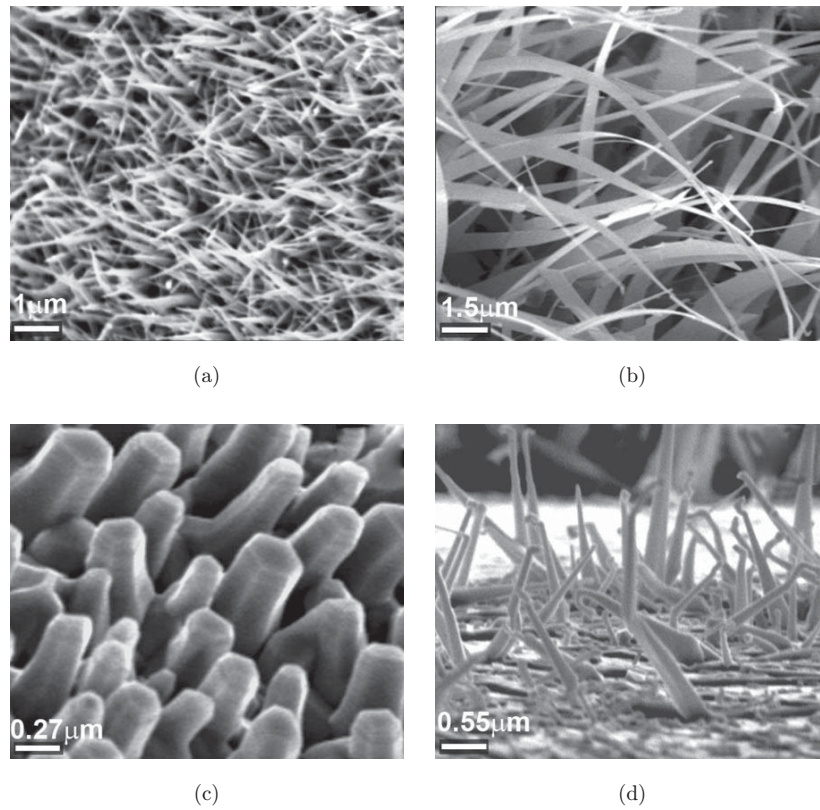


Fig. 1. SEM images (tilted view) of vertically aligned ZnO nanostructures: (a) nanowires, (b) nanoribbons and (c) nanorods grown at different temperatures using ZnO nanopowder as the source material; (d) nanowires grown at 750°C using ZnO bulk powder as the source, respectively.

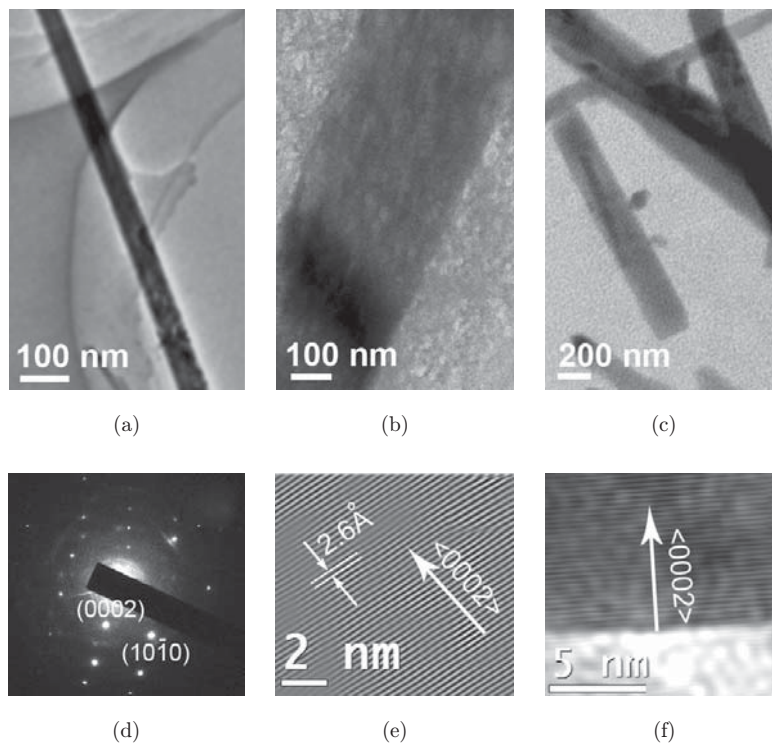


Fig. 2. TEM images of ZnO: (a) nanowires, (b) nanoribbons and (c) nanorods grown at different temperatures; (d) SAED pattern of the corresponding nanowire; (e) and (f) high resolution TEM images of the corresponding nanowire and nanorod, respectively. These nanostructures are grown along (0002) direction.

2.60 Å, equivalent to the spacing of (0002) planes in wurtzite ZnO crystal indicating growth along $\langle 0002 \rangle$ direction. The HRTEM and SAED results are consistent with the XRD results. These results are in good agreement with the previous reports.³⁻⁷

It is accepted that in catalyst mediated growth, ZnO nanowires and nanorods are grown by VLS mechanism⁸ and nanoribbons are grown by VS mechanism.⁹ Formation of varieties of ZnO nanostructures mainly controlled by growth temperature, surface energy of the growth plane and source material and zinc vapor pressure.⁷ In general, it is observed that temperature below 800°C is suitable for the growth of ZnO nanowires and above 800°C is suitable for the growth of ZnO nanorods. In our case, final shape of the as-grown nanostructures is controlled by growth temperature and Zn/ZnO_x vapor pressure. As high temperature region was nearer to the ZnO source, there was a large variation of zinc vapor pressure and ZnO_x concentration in different temperature regions. Due to ultrafine size of the ZnO nanopowder, during thermal evaporation the yield of vapor mixture (Zn, ZnO_x and CO) is too high. At high temperature region, which is nearer to the source material the supersaturation is low.⁷ That low supersaturation and high vapor pressure results in the growth of the nanorods rather than nanowires. In the present case depending upon the carrier gas flow rate and growth temperature, vapor mixture concentration and also supersaturation is maximum at ~850°C. Then, in this temperature vapor is deposited on the substrate in a fast rate and does not have sufficient time to react with the catalyst particles. The molecules have a good chance to diffuse to the front and the side surfaces. This deposition results in the growth of nanoribbons by

VS process. On the other hand, in the case ZnO bulk powder, yield of zinc vapor is relatively low. The Zn (ZnO_x) vapor sufficiently reacted with the gold particles during deposition. This deposition results in the growth of nanowires by VLS process.

The room temperature PL spectra of ZnO nanowires, nanoribbons and nanorods grown from ZnO nanopowder and nanowires grown from bulk powder are shown in Fig. 3, respectively. ZnO nanowires exhibit strong near band edge (NBE) UV emission at 380 nm and a broad green emission peak. On the other hand, nanoribbons and nanorods show relatively weak UV emission peak with same intensities at ~380 nm and an intense broad green emission peak. The green emission peak is deconvoluted by Gaussian line shape function to two peaks, one at ~500 nm and another at ~545 nm. The NBE emission is due to bound excitonic recombination and green emission at ~500 nm is attributed due to the recombination of photo-generated holes with the electrons belonging to oxygen vacancy states on the surface.¹⁰ And another green emission at ~545 nm is due to the presence of interstitial oxygen inside the nanostructure.¹¹ With increase in growth temperature, intensity of the ~500 nm emission peak is gradually increased to 3.12 times for the nanoribbons and 4.08 times for the nanorods. Whereas intensity of ~545 nm peak is increased 3.44 times for the nanoribbons and then decreased 2.17 times for the nanorods. And their intensity ratio is calculated as 0.89, 0.82 and 2.29 for the nanowires, nanoribbons and nanorods, respectively. In general, ZnO nanorods/nanoribbons are grown at higher temperature. Where, presence of oxygen vapor is relatively low compared to the low temperature region, which results in the formation of large no of oxygen vacancy states in the

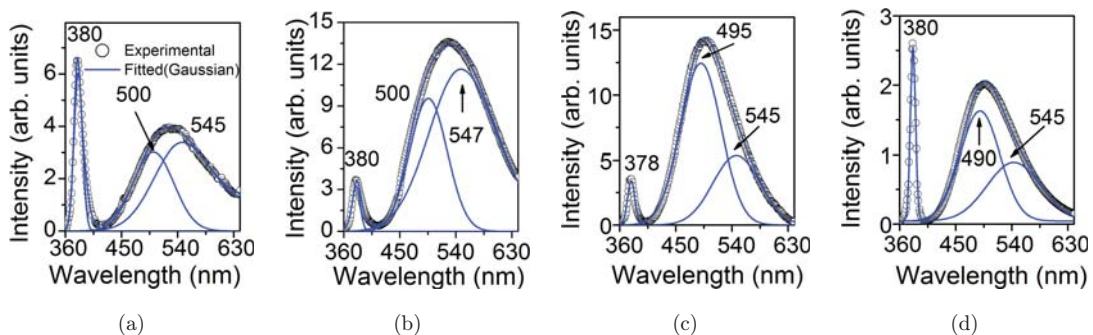


Fig. 3. Room temperature PL spectra of ZnO: (a) nanowires, (b) nanoribbons and (c) nanorods synthesized from ZnO nanopowder source material; (d) nanowires synthesized from bulk ZnO powder source material, respectively. Solid lines are the fitted line with Gaussian function to the experimental data.

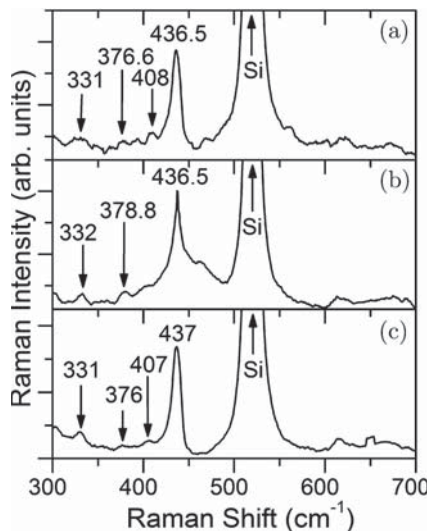


Fig. 4. Micro-Raman spectra of ZnO nanostructures: (a) nanowires, (b) nanoribbons and (c) nanorods.

ZnO nanorods/nanoribbons. As a result strong green emission is observed from the nanorods/nanoribbons.

Raman scattering studies of these nanostructure show good quality crystalline wurtzite structure. The peaks located at ~ 331 , ~ 376 , 407 and ~ 437 cm^{-1} in Fig. 4 correspond to the $2E_2$, $A_1(\text{TO})$, $E_1(\text{TO})$ and E_2^{high} phonon modes of wurtzite ZnO,¹² respectively. The strong Si peaks are coming from the substrate. The Raman spectra taken from the ZnO nanowires and nanorods (Figs. 4(a) and 4(c)) show four peaks with strong E_2^{high} mode, whereas only three peaks are observed for the nanoribbons grown at 750°C (Fig. 4(b)). The observed peaks of wurtzite ZnO phase are found to be red shifted (~ 1 cm^{-1}) due to the presence of a tensile strain in the as grown nanostructures.¹³ Quantum confinement effect is not dominant in this case due to their larger size as compared to exciton-bohr radius of ZnO.

4. Conclusion

We studied the effect of ZnO nanopowder source and growth temperatures on shape evolution of the

ZnO nanostructures. At lower growth temperature and lower zinc vapor pressure, nanowires were formed and with increase in growth temperature and vapor pressure nanoribbons and then nanorods were obtained. Due to the effect of ultrafine size of the ZnO nanoparticles and ultrathin gold layer on the Si substrate, we observed the formation of nanoribbons by VS process, while the nanowires and nanorods were formed by VLS process at different growth temperatures.

References

1. Z. L. Wang, *J. Phys.: Condens. Mater.* **16**, R829 (2004).
2. B. Gil and A. V. Kavokin, *Appl. Phys. Lett.* **81**, 748 (2002).
3. W. I. Park, J. S. Kim, G.-C. Yi and H.-J. Li, *Adv. Mater.* **17**, 1393 (2005).
4. M. H. Huang, S. Mao, H. Feick, H. Yan, Y. Wu, H. Kind, E. Weber, R. Russo and P. Yang, *Science* **292**, 1897 (2001).
5. Z. Fan and J. G. Lu, *Appl. Phys. Lett.* **86**, 123510 (2005).
6. M. Law, L. E. Green, J. C. Jhonson, R. Saykally and P. Yang, *Nat. Mater.* **4**, 455 (2005).
7. C. Ye, X. Fang, Y. Hao, X. Teng and L. Zhang, *J. Phys. Chem. B* **109**, 19758 (2005).
8. M. H. Huang, Y. Wu, H. Feick, N. Tran, E. Weber and P. Yang, *Adv. Mater.* **13**, 113 (2001).
9. Z. W. Pan, Z. R. Dai and Z. L. Wang, *Science* **291**, 1947 (2001).
10. K. Vanheusden, W. L. Warren, C. H. Seager, D. K. Tallant, J. A. Voigt and B. E. Gnade, *J. Appl. Phys.* **79**, 7983 (1996).
11. B. Lin, Z. Fu and Y. Jia, *Appl. Phys. Lett.* **79**, 943 (2001).
12. Ü. Özgür, Y. I. Alivov, C. Liu, A. Teke, M. A. Reshchikov, S. Doan, V. Avrutin, S.-J. Cho and H. Morkoç, *J. Appl. Phys.* **98**, 041301 (2005).
13. I. De Wolf, M. Ignat, G. Pozza, L. Maniguet and H. E. Maes, *J. Appl. Phys.* **85**, 6477 (1999).